Effects of nano-SiO$_2$ and glass powder on

mitigating alkali-silica reaction of cement glass mortars

Yamei Cai, Dongxing Xuan, Chi Sun Poon*
Department of Civil and Environmental Engineering
The Hong Kong Polytechnic University
Corresponding author: cecspoon@polyu.edu.hk

Abstract: Swelling caused by alkali-silica reaction (ASR) in concrete is a deleterious behavior due to reactions between alkaline pore solution and amorphous or metastable forms of silica in aggregates. Generally, mitigation by using pozzolanic materials is commonly adopted. This study compared the effectiveness of a highly-reactive nano-SiO$_2$ (NS) and a slowly-reactive waste glass powder (WGP) on mitigating ASR of cement mortars prepared with crushed glass cullet as aggregates. The experimental results showed that incorporating 2% NS or 10% WGP or a hybrid of the two in the mortar can decrease the ASR expansion. Using WGP resulted in larger reduction in the ASR expansion than using NS. Meanwhile, there was an improvement of strength from 7 d to 28 d for the mortar prepared with WGP. The composition of reaction products containing the ASR gel formed in a simulated ASR condition and the macro-/micro-structure of the tested mortars were further analyzed. It was found that the reaction products formed with high ratios of Na/Si and Ca/Si were favorable in mitigating the ASR expansion. For the specimen prepared with WGP, the increase in the ratio of Ca/Si would increase the stiffness of the ASR gel, and a higher Na/Si ratio would help reduce the osmotic pressure. The findings from this study would be useful for the selection of pozzolans to mitigate the ASR effect when using crushed glass cullet as aggregates in cement mortars.

Key words: Alkali-silica reaction; Nano-SiO$_2$; Waste glass powder; Waste glass cullet; Pozzolanic materials

1. Introduction

Alkali-silica reaction (ASR) is one of the challenging problems related to the durability of concrete. During the process of ASR, various metastable forms of silicate phases in the reactive aggregates are dissolved by the alkaline pore solution of concrete and form the ASR gel. This gel has a general composition of $(SiO_2) \cdot (Na_2O)_n \cdot (K_2O)_k \cdot (CaO)_c \cdot (H_2O)_x$, and typically falls into the range of 0.05-0.6 for $(Na_2O+K_2O)/SiO_2$ and 0-0.2 for $(CaO+MgO)/SiO_2$ (molar ratio) [1]. Due to its porous feature and many hydrophilic groups (e.g., -OH, -O….Na, and –O$^-$), the gel generates osmotic pressure, imbibe water and expands [2, 3]. Therefore, cracks in the vicinity of the reactive aggregates can be initiated and developed to deteriorate the concrete [3, 4].

In recent years, using waste glass cullet as a secondary aggregate in concrete has been promoted and this can provide an environmental friendly solution for the management of non-recyclable glass waste [5-10]. However, the deleterious ASR effect between glass cullet and the alkaline solution in concrete restricts its application in practice. To mitigate the ASR effect, a portion of cement was replaced by supplementary cementitious materials (SCMs), such as fly ash [4, 11-13], ground granulated blast furnace slag (GGBS) [11, 14] and silica fume [15, 16], which is one of the most effective methods. The mitigation effect of SCMs on ASR is mainly related to the dilution of alkalinity [17], consumption of calcium hydroxide (CH) [18] and alkali fixation by calcium silicate hydrates (C-S-H) [3, 19-21], which lead to the reduction of alkalinity in the pore solution.

However, a number of studies also reported that although some pozzolanic materials such as waste glass powder (WGP) [22-26] and nano-SiO$_2$ (NS) [27-29] can mitigate ASR, there was no reduction of alkalinity in the pore solution, especially at the early ages. The pozzolanic reaction of WGP increased the alkali concentration of pore solution due to the release of large amounts of alkali from the reacted glass [30]. As regards NS, the results from Hou et al. [31] showed that the addition of NS can increase the initial pH value of cement pastes due to the accelerated effect of NS on the dissolution of cement particles, and then there was no significant reduction of pH value due to the relatively lower level of pozzolanic reaction at a later stage. As shown in the results reported by Singh et al [32], after 15 hours of cement hydration, an increase of Ca^{2+} concentration in the pore solution of C$_3$S incorporating NS paste started again and gradually approached to that of the pure C$_3$S paste.

The research results from Zheng et al. [22] proposed another ASR mitigation mechanism of WGP that the increase of aluminum concentration in the pore solution could reduce the dissolution of silica from the reactive aggregates. Even so, the reasons why WGP can mitigate ASR are still unclear. For NS, the incorporation of 0-3% NS in concrete had little impact on ASR, but the exact mechanism had not been studied [27-29].

In this study, the effects of adding NS and WGP on mitigating the ASR expansion of cement mortars prepared with waste glass cullet as aggregates were investigated. The dosage used was 2% of NS and 10% of WGP, respectively. The relatively lesser percentage of NS used was due to the difficulty of dispersing higher dosages of NS [33-36] and lower cost. Also, a relatively low dosage of NS has a great potential to improve the durability of concrete such as mechanical properties [35, 37] and transport properties [38]. The ASR expansions of the prepared mortars were

measured based on the accelerated mortar bar test. Also, the impacts of ASR on cement glass mortars were evaluated by measuring their bulk electrical resistance, compressive strength and pore structures. Furthermore, the composition of reaction products containing the ASR gel and wrapping WGC particles formed in a simulated ASR condition and the micro-/macro-structure of the tested mortars were analyzed to explain the effectiveness of NS and WGP on mitigating ASR.

2. Materials and experimental methods

2.1 Materials

Ordinary Portland cement (OPC: 52.5) was used in this study. WGP was obtained by a ball milling process of recycled waste glass cullet and waste glass cullet (WGC) was derived from crushing recycled beverage bottles. A commercially available NS powder with a particle size distribution in the range of 7-40 nm (Aladdin Industrial Corporation) was used. X-ray fluorescence analyzer (XRF, Rigaku Supermini 200) was used to evaluate the chemical compositions of cement, WGP and NS. A BET-N_2 adsorption instrument (ASAP 2020 Plus, micrometrics) was used to measure the BET surface areas of these materials. These parameters are given in Table 1. The BET surface area of NS was much higher than that of WGP (296,000 m^2/kg vs. 485 m^2/kg). The particle size distributions of OPC and WGP are shown in Fig.1. WGP used was slightly finer than OPC.

WGC was washed and dried at 105°C for 2 d and then cooled down to room temperature before it was used in the mortar as aggregates. Particles larger than 5 mm were removed.

2.2 Preparation of cement glass mortar specimens

Cement glass mortars were prepared with a water/binder ratio (w/b) and a binder/aggregate (glass cullet) ratio of 0.5 and 1/3, respectively. A commercial

naphthalene sulfonate superplasticizer (SP) with a solid content of 43% was used to achieve a similar fluidity for all prepared mortars. When 2% NS was added, 1.8% SP was needed to obtain a similar workability. The mix proportions of materials used are listed in Table 2.

In order to well disperse NS in water, a bath sonicator was used. NS was first added into water and stirred for 1 min, and then was sonicated for another 10 min before using in the mortar.

During the process of preparing cement mortars, cement and WGC were first dry-mixed for 1 min at a speed of 121 rpm, and then water or NS suspension or WGP was added. These blended materials were further mixed at a speed of 218 rpm for 2 min and then at a speed of 489 rpm for another 2 min. After mixing, the fresh mortar was cast into steel molds with dimensions of 40 mm × 40 mm × 160 mm, 25 mm × 25 mm × 285 mm and 40 mm × 40 mm × 40 mm respectively, and then a plastic sheet was used to cover the surface of the samples for 24 h before demolding.

2.3 Simulated ASR test

In order to further understand the effects of NS and WGP on the compositions of reaction products containing ASR gel formed in cement glass mortars, simulated ASR experiments by using different mixtures were designed and prepared. The mix proportions are shown in Table 3.

As seen in Table 3, this system simulated the formation of ASR gel around the WGC aggregates. In this test, cleaned WGC aggregates with a particle size of about 5 mm were used. WGC, calcium hydroxide (CH), NS or WGP were placed in polyethylene bottles. Then 200 mL of 1 N NaOH solution was added and these bottles were sealed and placed in a water bath at 80 ºC for 3 d, 7 d, 14 d and 28 d. At the end of each period, the reaction products formed on the surface of each WGC were

carefully washed off by deionized water, and then these WGC was removed from the solution. After that, all solid reaction products left in the bottles were collected by using a centrifuge. Then these solid reaction products were immersed in ethanol for 2 d before vacuum-dried at 60 ℃ for 2 d. Then these samples were ground to smaller than 74 μm for different tests such as the residual CH contents and the compositions of the reaction products.

2.4 Experimental methods

2.4.1 Measurement of ASR expansion

The expansion of mortars was tested by an accelerated ASR method in accordance with a modified version of ASTM C1260-14 [39]. The samples with dimensions of 25 mm × 25 mm × 285 mm were placed in a water bath at 80 ℃ for 24 h after demolding. After recording the initial length of mortars, they were immersed in a 1 N NaOH solution at 80 ℃ for 14 d. The expansion values of samples were measured periodically and the average of four samples was taken as a representative value.

2.4.2 Determination of bulk electrical resistance

Electrochemical impedance spectroscopy (EIS) was used to characterize the change of bulk electrical resistance of cement mortar (40 mm × 40 mm × 40 mm) during the accelerated ASR test at 3 d, 7 d and 14 d. This non-destructive measurement can monitor the in-situ variation of bulk electrical resistance in relation to the development of pore structure and micro-/macro-cracks in the cementitious materials [40, 41]. An increase of resistance indicates a dense microstructure and vice versa. EIS measurement was conducted by a Multi-Autolab M 204 device with a frequency range from 1 Hz to 1 MHz with a 10 mV AC signal magnitude. All experiments were performed using a two-electrode system and the schematic diagram

of equipment setup is illustrated in Fig. 2. In order to ensure proper electrical contacts between the specimen and the electrodes, a thin wet sponge was placed between them.

Fig. 3 shows a typical Nyquist curve obtained from the EIS test. It is composed of the real and imaginary impedances at different frequencies. In general, the impedance spectrum consists of a high frequency arc (bulk arc) and a low frequency arc (electrode arc), which are associated with the bulk electrical properties of cementitious materials and the polarization effect of electrode/specimen, respectively. For the Nyquist curve, the intersection value of bulk arc and electrode arc in the x-axis can be defined as bulk electrical resistance (R_b) [42].

2.4.3 Measurement of compressive strength

The equivalent compressive strength of cement mortars (40 mm × 40 mm × 160 mm) after exposed to the accelerated-ASR test for 3 d, 7 d and 28 d were measured according to BS EN 1015-1111:2007 [43]. The average values of six samples are reported.

2.4.4 Crack detection

The cement mortars (25 mm × 25 mm × 285 mm) were exposed to the accelerated ASR test for 28 days, then cracks, if any, were observed using an optical microscope with a magnification of 75. The crack width was measured and the photographs of the cracks were recorded.

2.4.5 Determination of pore structure

Mercury intrusion porosimetry (MIP) (Micromeritics Instrument Corporation, USA) was used to evaluate pore size distribution and porosity of cement mortars that were exposed to the accelerated ASR test for 7 d and 28 d. The specimens were fractured into small granular particles and immersed in ethanol for 2 d to terminate the

hydration of cement. Then these samples were vacuum-dried at 60 °C for 2 d before MIP tests.

2.4.6 Determination of calcium hydroxide content

Thermogravimetric analysis (TGA) was used to measure the residual CH contents in the simulated ASR system (as shown in Table 3). The collected powder sample was heated in an argon atmosphere from 25 °C to 850 °C at a rate of 10 °C/min using a TG/DTA 8121 analyzer (Rigaku, Japan). CH content can be calculated according to the method developed by Olek and Kim [44].

2.4.7 Microstructure analysis by SEM

The microstructures of mortars experienced to the accelerated ASR test for 28 d were observed by a scanning electron microscope (SEM). The SEM device was equipped with an energy dispersive X-ray (EDS) detector (TESCAN VEGA3). The analysis was performed in a backscattered electron (BSE) mode. Moreover, the collected reaction products (in powder form) from the simulated ASR tests (Section 2.3) were analyzed by the SEM/EDS.

3. Results and discussion

3.1 Influence of NS and WGP on ASR expansion

Fig. 4 shows the expansion values of mortar bars experienced to the accelerated ASR test for 14 d. Compared to the control sample, there was a reduction in the expansion of the mortars prepared with 2% NS or 10% WGP. The reduction level of the mortars prepared with 10% WGP (57% at 14 d) was the highest, followed by that prepared with a hybrid of 2% NS and 10% WGP (44% at 14 d), and the least reduction level of 23% was found for the mortars prepared with 2% NS. The relative ineffectiveness of NS was consistent with the previous findings reported by

Mukhopadhyay [28] and Zeidan [27] who found that 0.5% and 3% NS were not effective to reduce the ASR expansion.

3.2 Evolution of bulk electrical resistance of the tested mortars

The Nyquist diagrams of the different tested mortars are shown in Fig. 5. For the control mortar (Fig. 5(a)) and the mortar incorporated with 2% NS (Fig. 5(b)) subjected to the accelerated ASR test for 3 d, 7 d and 14 d, the impedance spectra in the complex plane gradually shifted to the left, and bulk electrical resistance (R_b) continuously decreased with the increase of alkaline solution immersion days. Comparing the mortars prepared with 10% WGP (Figs. 5(c)) or a hybrid of 10% WGP and 2% NS (Fig. 5(d)), it can be noticed that there was an opposite trend, and a noticeable increase in R_b occurred in the same immersion days.

Fig. 6 further shows the change of R_b at different alkaline immersion days compared to that at 3 d. For the control mortar and the mortar prepared with 2% NS, their reduction in R_b was comparable. However, for the mortar prepared with 10% WGP, there was a considerable increase in R_b value by 58 % and 75% at 7 d and 14 d respectively. For the mortar prepared with a hybrid of 2% NS and 10% WGP, the increase in R_b was less than that of mortar prepared with 10% WGP (25% at 7 d and 33% at 14 d).

For the control mortar and the mortar prepared with NS, the reduction in R_b would be linked to the presence of more microcracks due to the larger ASR expansion. When compared with the mortar prepared with 10% WGP and the mortar prepared with a hybrid of 2% NS and 10% WGP, there was an increase in R_b, which would be related to the lesser amount of microcracks. It is believed that large ASR expansion would cause more cracks [45, 46]. These cracks could make the discontinuous paths change into continuous ones [40, 41], which would then create the preferential

9

pathways for pore solution penetration, which resulted in the reduction of the bulk electrical resistance. It can be noticed that, for the mortar incorporated with a hybrid of 2% NS and 10% WGP, there was a smaller increase in R_b than that of the mortar prepared with 10% WGP. This result was consistent with ASR expansion results.

3.3 Influence of NS and WGP on compressive strength

Compressive strength values of the tested mortars are shown in Fig. 7. For all mortars, there was a slight increase in compressive strength from 3 d to 7 d of alkaline immersion. However, from 7 d to 28 d, only the mortar prepared with 10% WGP experienced an increase in strength. A large decrease in the compressive strength for the mortars prepared with NS after subjecting to the accelerated ASR test was also reported by Zeidan et al. [27]. It can be seen that the increase in the compressive strength of mortars from 3 d to 7 d should be attributed to the continuous hydration of cementitious materials. After 7 d, ASR expansion would start to significantly influence the strength development. When micro-/macro-cracks had developed to certain extend, they could cause a significant decrease of compressive strength. But a smaller expansion and continuous pozzolanic reaction of the mortar prepared with 10% WGP resulted in a continuous increase of compressive strength.

Furthermore, for the mortar prepared with 10% WGP, lower compressive strength at 3 d and 7 d were found when compared with the control due to lower reactivity of WGP. This would result in higher porosity of mortar. The gel formed during ASR process would have opportunities to fill bigger pores, which might decrease the swelling pressure caused by ASR gel [2]. However, when the highly reactive NS was used, compressive strength was greatly increased in the first 3 d due to the fast pozzolanic reaction [47] and seeding effect of NS [32]. But no further increase in strength was observed for the 2% NS sample after 3 d, the reason could be

ascribed to that majority of NS had been reacted within the first 3 d. For the hybrid specimens (10% WGP + 2% NS), there was a progressive increase of strength from 3 d to 7 d due to the slow pozzolanic reaction of WGP. For the samples prepared with NS, the denser structure would lead to a lower porosity, which cannot accommodate the swelling pressure of ASR gel leading to more significant deterioration of mortars after 7 d of immersion in the alkaline environment.

3.4 Pore structure

Fig. 8 shows the pore structure development of mortars after subjecting to the accelerated ASR test for 7 d and 28 d. The reduction in total porosity of the tested mortars from 7 d to 28 d was approximately 0.27 %, 1.06 %, 1.98 % and 1.62 % for the control mortar, the mortar prepared with 2% NS, the mortar prepared with 10% WGP and the mortar prepared with the hybrid of WGP and NS, respectively. The smallest reduction was observed for the control mortar and the highest reduction due to the pore refinement effect was shown in the mortar prepared with 10% WGP.

3.5 Effect of ASR on the macro-/micro-structure

Fig. 9 shows the BSE images and crack photos of mortars after exposed to the accelerated ASR condition for 28 d. More obvious ASR gel and wider cracks can be observed in the control mortar. There were some narrower ASR gel and relatively narrower cracks in the mortar incorporated with 2% NS (Fig. 9 (b)). In comparison, no noticeable ASR gel and the narrowest cracks were observed in the mortar prepared with 10% WGP in Fig. 9 (c). These results confirmed that WGP was effective for the mitigation of ASR.

3.6 Consumption of CH in the simulated ASR test

A simulated accelerated ASR test method was conducted in order to reduce the interference of other constituents in the system. The aim of this experiment was to

analysis the effect of NS or WGP on the consumption of CH as well as on the composition changes of the formed reaction products containing ASR gel. It has been reported that the formation of the ASR gel needs the presence of CH or soluble Ca^{2+} ions [3, 18, 48]. Therefore, a comparison of the consumption of CH by TGA in the system should be able to evaluate the effectiveness of NS or WGP on suppression ASR. The results are shown in Fig. 10.

It was found that there was a continuous consumption of CH in the control specimen. For the other specimens, there was a significant increase in the CH consumption during the first 7 d. After 7 d, for the specimens prepared with WGP and a hybrid of NS and WGP, much slower consumption of CH was noticed. In contrast, for the specimens prepared with NS, there was a rapid linear increase of consumption after 7 d.

For the control specimen, the continuous consumption of CH showed that ASR occurred and the corresponding ASR gel was formed continuously. For the other specimens, before 7 d, the increasing consumption of CH should be mainly attributed to the pozzolanic reaction of the respective materials owing to the quick chemical reactions caused by the high surface area of the small WGP and NS. After 7 days, for the specimens incorporated with WGP and the specimen prepared with NS and WGP, slower consumptions of CH could be due to the larger size of WGC and the dense structure of the formed reaction products (e.g., ASR gel) wrapping the WGC particles. For the mortar prepared with NS, a significant increase of consumed CH started again after 7 days, which could be due to the different composition and properties of ASR gel formed around glass cullet. The possible reasons will be further discussed in Section 3.7.

3.7 Compositions of reaction products wrapping WGP particles in the simulated ASR test

The ratios of Na/Si and Ca/Si in the different reaction products containing ASR gel formed in the simulated ASR test for 28 d were calculated based on the results of EDS, and during the calculation process, the non-reacted CH had been deducted. These results are listed in Table 4. For the control specimen, relatively lower Na/Si (0.34) and Ca/Si (0.43) ratios were found in the formed reaction products. For the specimens prepared with NS or WGP, there were an increase in the Na/Si ratio. For the specimen prepared with WGP, it had the highest ratio of Ca/Si (1.03). In comparison, for the specimen prepared with a hybrid of NS and WGP, the formed products had a lower ratio of Ca/Si than those prepared with the incorporation of NS or WGP alone, but a higher Na/Si ratio than all the other samples. Taking into account the deleterious impacts on the strength and porosity of the tested mortars (as shown in Figs. 4-8), it can be concluded that the reaction products wrapping WGC particles with higher ratios of Na/Si and Ca/Si would induce less damages.

It is known that the reaction products from ASR with a very low Ca content and a high alkali (Na, K) content would be flowable and able to permeate through the pore structure of materials. Thus less swelling pressure is generated to induce damages to the matrix [2, 49]. However, the alkali ions in the reaction products can be replaced by the presence of Ca (called "alkali recycling") [3]. When the reaction product has an appropriate Ca content, the ASR gel would be formed, bearing many hydrophilic groups (e.g., -OH, -O...Na, -O$^-$). As a result, adsorption of water and swelling of ASR gel would occur. If a rich Ca ion environment still exists in the pore solution, calcification can further occur and ASR gels would become stiffer and more difficult to flow. It was reported [2, 3] that if the molar ratio of Ca/Si was higher than 0.5, the

formed ASR gel had a high stiffness and low expansion, and the composition and properties of ASR gels would gradually approach to that of the pozzolanic C-S-H. Therefore, the Ca/Si ratio in the ASR gel can significantly affect the expansive behavior.

Furthermore, the ASR gel formed around WGC particles could act as a semi-permeable membrane, allowing smaller ions (e.g., Na^+ and OH^-) to pass through, while the larger ions (e.g., silicate) cannot [3]. This results in the formation of osmotic pressure [3]. It was reported that the Na/Si ratio had an important impact on the osmotic pressure of the ASR gel containing a high Ca content and the gel's viscosity [2, 3]. A high ratio of Na/Si is favorable in reducing the swelling and potential ASR damage. When compared with the compositions of reaction products formed in the control and the hybrid specimens in Table 4, it can be found that high Na/Si would be helpful to reduce the expansion. It was also noticed that even though high Na content provided a better flowability, the lower Ca/Si ratios of the specimen prepared with both WGP and NS could increase the potential expansion due to its lower stiffness as proposed by previous studies [2, 3].

4. Conclusions

This study presented the effects of highly-reactive NS and slow-reactive WGP on the mitigation of ASR, the evolution of bulk electrical resistance, the development of compressive strength and pore structure of glass cement mortars. In relation to these deleterious impacts, the composition of reaction products containing ASR gel formed in a simulated ASR test and the macro-/micro-structure of the tested mortars were further analyzed. From this work, the following findings can be summarized:

- The incorporation of 2% NS and 10% WGP in cement glass mortars can reduce the ASR expansion by different degrees. The mitigation effectiveness

14

of 2% NS was lower than 10% WGP. When a hybrid of 2% NS and 10% WGP was incorporated, the mitigation effect was inferior to that of the mortar with 10% WGP as well.

- For the control cement glass mortar and the mortar prepared with 2% NS, there was a reduction in bulk electrical resistance (R_b) value due to the presence of more microcracks caused by larger ASR expansion. However, for the mortars prepared with 10% WGP and prepared with a hybrid of 2% NS and 10% WGP, there was an increase in the R_b value, and a higher increase in the R_b value was found for the mortar prepared with 10% WGP, which can be attributed to the lesser amount of microcracks due to the lower expansion.

- When the mortars were exposed to the accelerated ASR test, except for the sample prepared with 10% WGP, obvious reductions in compressive strength were noticed from 7 d to 28 d, which was due to the deterioration of mortar microstructure. However, the increase in compressive strength for the mortar prepared with 10% WGP from 7 d to 28 d could be due to the smaller expansion and continuous pozzolanic reaction.

- Based on the results of the simulated ASR test, the formed reaction products containing ASR gel and wrapping WGC particles with high Na/Si and Ca/Si ratios were favorable in mitigating the ASR expansion. For the specimens prepared with WGP, the increase of Ca/Si ratio increased the stiffness of ASR gel, and a higher Na/Si ratio would help reduce the osmotic pressure of ASR gel. The composition of ASR gel played an important role on the deleterious effect of expansion on matrix.

15

References

[1] X.Q. Hou, R.J. Kirkpatrick, L.J. Struble, P.J.M. Monteiro, Structural Investigations of Alkali Silicate Gels, J. Amer. Ceram. Soc. 88(4) (2005) 943-949.

[2] A. Gholizadeh Vayghan, F. Rajabipour, J.L. Rosenberger, Composition–rheology relationships in alkali–silica reaction gels and the impact on the gel's deleterious behavior, Cem. Concr. Res. 83 (2016) 45-56.

[3] F. Rajabipour, E. Giannini, C. Dunant, J.H. Ideker, M.D.A. Thomas, Alkali–silica reaction: Current understanding of the reaction mechanisms and the knowledge gaps, Cem. Concr. Res. 76 (2015) 130-146.

[4] S.M.H. Shafaatian, A. Akhavan, H. Maraghechi, F. Rajabipour, How does fly ash mitigate alkali–silica reaction (ASR) in accelerated mortar bar test (ASTM C1567)? Cem. Concr. Compos. 37 (2013) 143-153.

[5] N. Schwarz, N. Neithalath, Influence of a fine glass powder on cement hydration: Comparison to fly ash and modeling the degree of hydration, Cem. Concr. Res. 38(4) (2008) 429-436.

[6] E.J. Garboczi, K.A. Riding, M. Mirzahosseini, Particle shape effects on particle size measurement for crushed waste glass. Adv. Powder Technol. 28(2) (2017) 648-657.

[7] C. Shi, K. Zheng, A review on the use of waste glasses in the production of cement and concrete, Resources, Conserv. Recycl. 52(2) (2007) 234-247.

[8] C.H. Chen, R. Huang, J.K. Wu, C.C. Yang, Waste E-glass particles used in cementitious mixtures, Cem. Concr. Res. 36(3) (2006) 449-456.

[9] M. Aly, M.S.J. Hashmi, A.G. Olabi, M. Messeiry, A.I. Hussain, Effect of nano clay particles on mechanical, thermal and physical behaviours of waste-glass cement mortars, Mater. Sci. Eng. A, 528(27) (2011) 7991-7998.

[10] M.B.A. Alhasanat, A.N. Al Qadi, S. Al-Thyabat, M. Haddad, B.G. Nofal, Addition of Waste Glass to Self-Compacted Concrete: Critical Review, Modern Appl. Sci. 10(11) (2016) 1.

[11] S. Kandasamy, M.H. Shehata, The capacity of ternary blends containing slag and high-calcium fly ash to mitigate alkali silica reaction, Cem. Concr. Compos. 49 (2014) 92-99.

[12] M. Thomas, The effect of supplementary cementing materials on alkali-silica reaction: A review, Cem. Concr. Res. 41(12) (2011) 1224-1231.

[13] D.X. Xuan, P. Tang, C.S. Poon, Effect of casting methods and SCMs on properties of mortars prepared with fine MSW incineration bottom ash, Constr. Build. Mater. 167 (2018) 890-898.

[14] M. Mahyar, S.T. Erdoğan, M. Tokyay, Extension of the chemical index model for estimating Alkali-Silica reaction mitigation efficiency to slags and natural pozzolans, Constr. Build. Mater. 179 (2018) 587-597.

[15] A.J. Maas, J.H. Ideker, M.C.G. Juenger, Alkali silica reactivity of agglomerated silica fume, Cem. Concr. Res. 37(2) (2007) 166-174.

[16] W. Aquino, D.A. Lange, J. Olek, The influence of metakaolin and silica fume on the chemistry of alkali–silica reaction products, Cem. Concr. Compos. 23(6) (2001) 485-493.

[17] S. Diamond, Effects of two Danish flyashes on alkali contents of pore solutions of cement-flyash pastes, Cem. Concr. Res. 11(3) (1981) 383-394.

[18] S. Chatterji, The role of Ca (OH)$_2$ in the breakdown of Portland cement concrete due to alkali-silica reaction. Cem. Concr. Res. 9(2) (1979) 185-188.

[19] J. Duchesne, M-A. Bérubé, Long-term effectiveness of supplementary cementing materials against alkali–silica reaction, Cem. Concr. Res. 31(7) (2001) 1057-1063.

[20] H. Maraghechi, F. Rajabipour, C.G. Pantano, W.D. Burgos, Effect of calcium on dissolution and precipitation reactions of amorphous silica at high alkalinity, Cem. Concr. Res. 87 (2016) 1-13.

[21] X. Hou, L.J. Struble, R.J. Kirkpatrick, Formation of ASR gel and the roles of C-S-H and portlandite, Cem. Concr. Res. 34(9) (2004) 1683-1696.

[22] K. Zheng, Pozzolanic reaction of glass powder and its role in controlling alkali–silica reaction, Cem. Concr. Compos. 67 (2016) 30-38.

[23] H. Du, K.H. Tan, Use of waste glass as sand in mortar: Part II – Alkali–silica reaction and mitigation methods, Cem. Concr. Compos. 35(1) (2013) 118-126.

[24] K. Afshinnia, P.R. Rangaraju, Influence of fineness of ground recycled glass on mitigation of alkali–silica reaction in mortars, Constr. Build. Mater. 81 (2015) 257-267.

[25] J-X. Lu, B-J. Zhan, Z-H. Duan, C.S. Poon, Using glass powder to improve the durability of architectural mortar prepared with glass aggregates, Mater. Des. 135 (2017) 102-111.

[26] S. Guo, Q. Dai, X. Sun, X. Xiao, R. Si, J. Wang, Reduced alkali-silica reaction damage in recycled glass mortar samples with supplementary cementitious materials, J. Cleaner Prod. 172 (2018) 3621-3633.

[27] M. Zeidan, A.M. Said, Effect of colloidal nano-silica on alkali–silica mitigation, J. Sustain. Cement-Based Mater. 6(2) (2016) 126-138.

[28] A.K. Mukhopadhyay, K-W. Liu, Application of Nanotechnology to Control ASR in Portland Cement Concrete, Nanotechnol. Constr. (2015) 465-471.

[29] M. Aly, M.S.J. Hashmi, A.G. Olabi, M. Messeiry, E.F. Abadir, A.I. Hussain, Effect of colloidal nano-silica on the mechanical and physical behaviour of waste-glass cement mortar, Mater. Des. 33 (2012) 127-135.

[30] R. Idir, M. Cyr, A. Tagnit-Hamou, Use of fine glass as ASR inhibitor in glass aggregate mortars, Constr. Build. Mater. 24(7) (2010) 1309-1312.

[31] P. Hou, S. Kawashima, D. Kong, D.J. Corr, J. Qian, S.P. Shah, Modification effects of colloidal nanoSiO$_2$ on cement hydration and its gel property, Compos. Part B: Eng. 45(1) (2013) 440-448.

[32] L.P. Singh, S.K. Bhattacharyya, S.P. Shah, G. Mishra, U. Sharma. Studies on early stage hydration of tricalcium silicate incorporating silica nanoparticles: Part II, Constr. Build. Mater. 102 (2016) 943-949.

[33] D. Kong, X. Du, S. Wei, H. Zhang, Y. Yang, S.P. Shah, Influence of nano-silica agglomeration on microstructure and properties of the hardened cement-based materials, Constr. Build. Mater. 37 (2012) 707-715.

[34] H. Li, H-G. Xiao, J. Yuan, J. Ou, Microstructure of cement mortar with nano-particles, Compos. Part B: Eng. 35(2) (2004) 185-189.

[35] Z. Rong, W. Sun, H. Xiao, G. Jiang, Effects of nano-SiO$_2$ particles on the mechanical and microstructural properties of ultra-high performance cementitious composites, Cem. Concr. Compos. 56 (2015) 25-31.

[36] H. Madani, A. Bagheri, T. Parhizkar, The pozzolanic reactivity of monodispersed nanosilica hydrosols and their influence on the hydration characteristics of Portland cement, Cem. Concr. Res. 42(12) (2012) 1563-1570.

[37] H. Du, S. Du, X. Liu, Durability performances of concrete with nano-silica, Constr. Build. Mater. 73 (2014) 705-712.

[38] H. Du, S. Du, X. Liu, Effect of nano-silica on the mechanical and transport properties of lightweight concrete, Constr. Build. Mater. 82 (2015) 114-122.

[39] C. ASTM, 1260 Standard test method for potential alkali reactivity of aggregates (mortar-bar method), Section, 4 (2007) 676-680.

[40] T. Shi, L. Zheng, X. Xu, Evaluation of alkali reactivity of concrete aggregates via AC impedance spectroscopy, Constr. Build. Mater. 145 (2017) 548-554.

[41] G. Song, Equivalent circuit model for AC electrochemical impedance spectroscopy of concrete, Cem. Concr. Res. 30(11) (2000) 1723-1730.

[42] D. Ravikumar, N. Neithalath, An electrical impedance investigation into the chloride ion transport resistance of alkali silicate powder activated slag concretes, Cem. Concr. Compos. 44 (2013) 58-68.

[43] C.E. De Normalization, Methods of test for mortar for masonry–Part 11: determination of flexural and compressive strength of hardened mortar, UNI EN, Brussels, Belgium, (2007) 1015-1111.

[44] J. Olek, T. Kim, Effects of Sample Preparation and Interpretation of Thermogravimetric Curves on Calcium Hydroxide in Hydrated Pastes and Mortars, Transportation Research Record: Journal of the Transportation Research Board. 2290 (2012) 10-8.

[45] L.F.M. Sanchez, T. Drimalas, B. Fournier, D. Mitchell, J. Bastien, Comprehensive damage assessment in concrete affected by different internal swelling reaction (ISR) mechanisms, Cem. Concr. Res. 107 (2018) 284-303.

[46] R.A. Barbosa, S.G. Hansen, K.K. Hansen, L.C. Hoang, B. Grelk, Influence of alkali-silica reaction and crack orientation on the uniaxial compressive strength of concrete cores from slab bridges, Constr. Build. Mater. 176 (2018) 440-451.

[47] P. Hou, J. Qian, X. Cheng, S.P. Shah. Effects of the pozzolanic reactivity of nanoSiO$_2$ on cement-based materials, Cem. Concr. Compos. 55 (2015) 250-258.

[48] R.F. Bleszynski, M.D. Thomas, Microstructural studies of alkali-silica reaction in fly ash concrete immersed in alkaline solutions, Adv. Cem. Based Mater. 7(2) (1998) 66-78.

[49] M. Kawamura, K. Iwahori, ASR gel composition and expansive pressure in mortars under restraint, Cem. Concr. Compos. 26(1) (2004) 47-56.

Table 1 Oxide compositions and physical properties of cement, WGP and NS

ID	Cement (wt%)	WGP (wt%)	NS(wt%)
Oxide compositions			
CaO	62.01	11.23	\
SiO_2	19.26	69.29	99.30
Al_2O_3	7.19	2.18	\
Fe_2O_3	3.26	0.50	\
MgO	2.10	1.32	\
SO_3	1.99	0.22	\
K_2O	0.31	0.81	0.70
Na_2O	0.13	12.66	\
others	1.94	0.58	\
LOI	1.81	1.21	\
Physical properties			
BET surface area (m^2/kg)	1433	485	296,000

Table 2 Mix proportions of cement mortars (%)
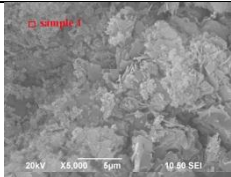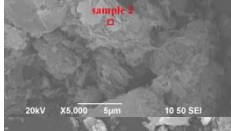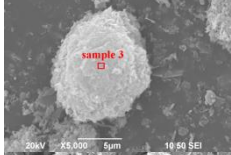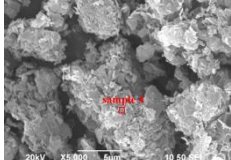
Sample ID	Cement	NS	WGP	Mortar SP*/B*
Control	100	0	0	0
2% NS	98	2	0	1.8
10% WGP	90	0	10	0
2% NS+10% WGP	88	2	10	1.8

Note: NS: nano-SiO$_2$, WGP: waste glass powder, SP*: the solids content of

superplasticizer, B*: binder=cement+NS+WGP

Table 3 Mix proportions of specimens

Sample ID	Glass cullet/g	CH/g	NS/g	WGP/g	1N NaOH/mL
Control	5	0.75	0	0	200
2% NS	5	0.75	0.1	0	200
10% WGP	5	0.75	0	0.5	200
2% NS+10% WGP	5	0.75	0.1	0.5	200

Table 4 Morphologies of reaction products (in powder form) and Na/Si and Ca/Si ratios

Code	SEM/EDS	Na/Si	Ca/Si
Control		0.34	0.43
2% NS		0.45	0.75
10% WGP		0.46	1.03
2% NS+10% WGP		0.59	0.56
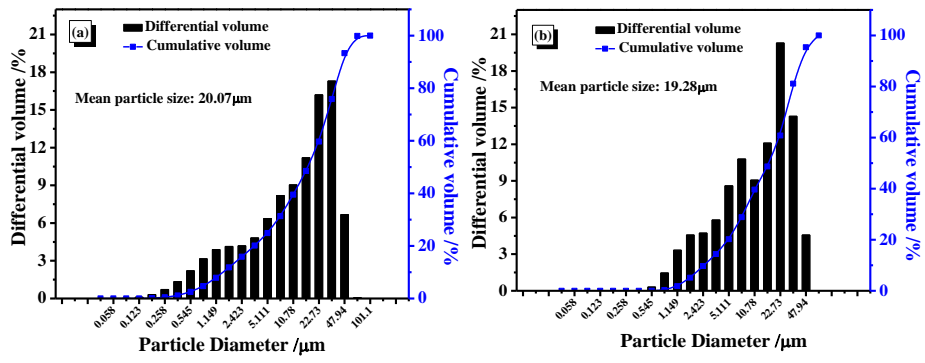
Fig. 1 The particle size distribution of cement (a) and waste glass powder (b)
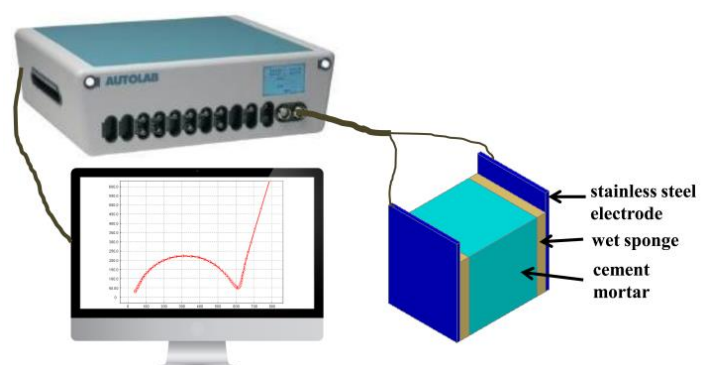
Fig. 2 Schematic diagram of two-point EIS measurement setup
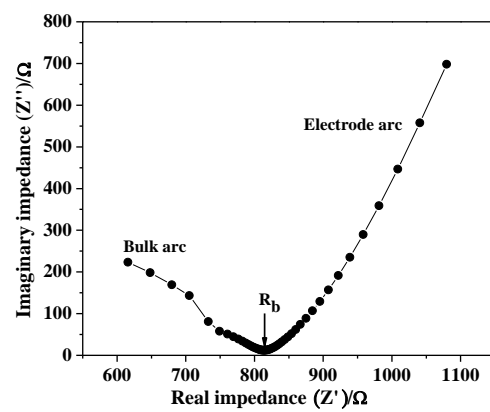
Fig. 3 A typical Nyquist curve obtained from EIS
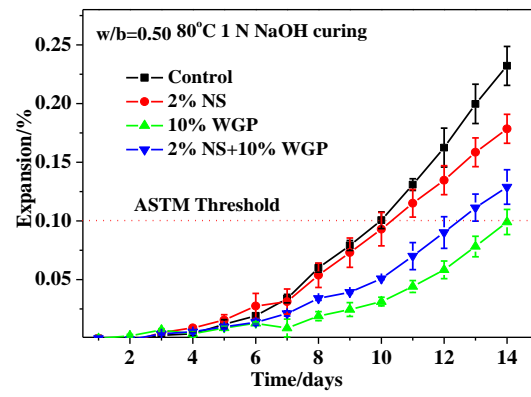
Fig. 4 Expansion of mortar bars exposed to the accelerated ASR test
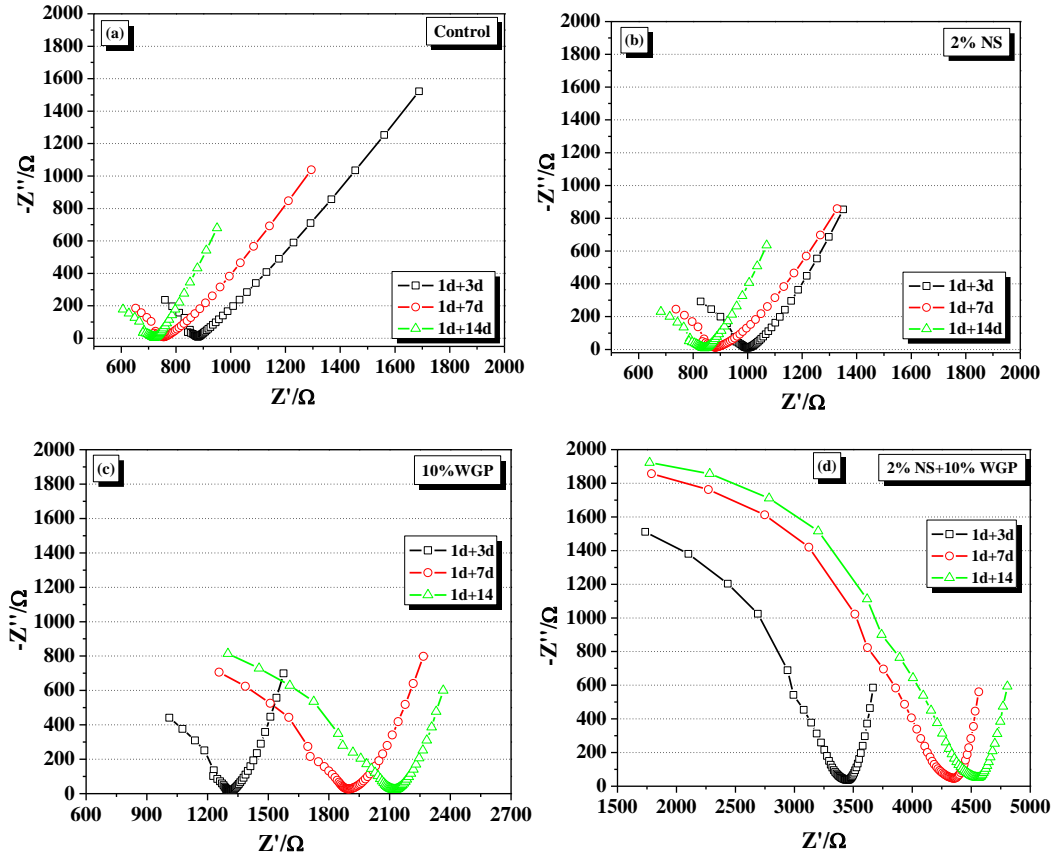
Fig. 5 Nyquist diagrams of mortars experienced to the ASR test ((1 d+3 d), (1 d+7 d) and (1 d+14 d) mean mortars were cured in water at 80ºC for 1 d, and then cured in 1N NaOH solution 80ºC for 3 d, 7 d and 14 d.)
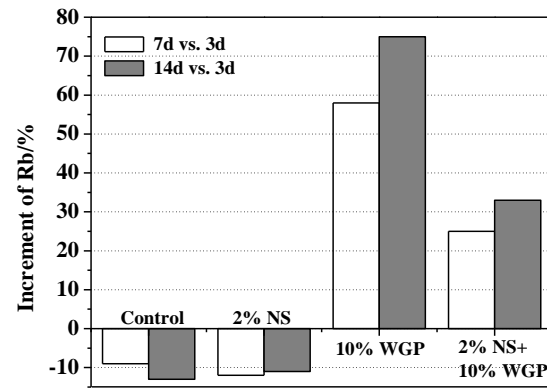
Fig. 6 Increment of R_b determined by EIS test
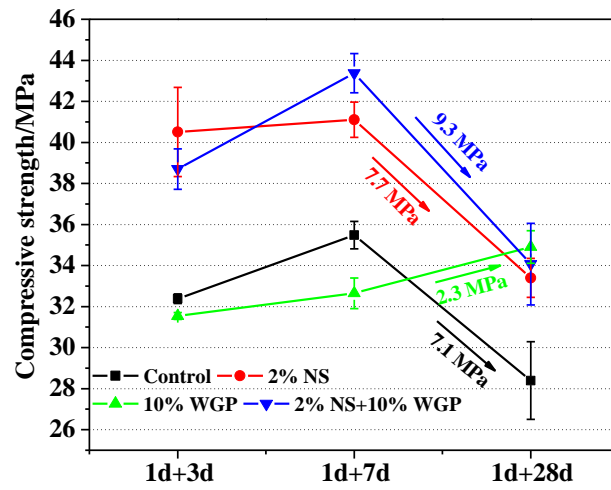
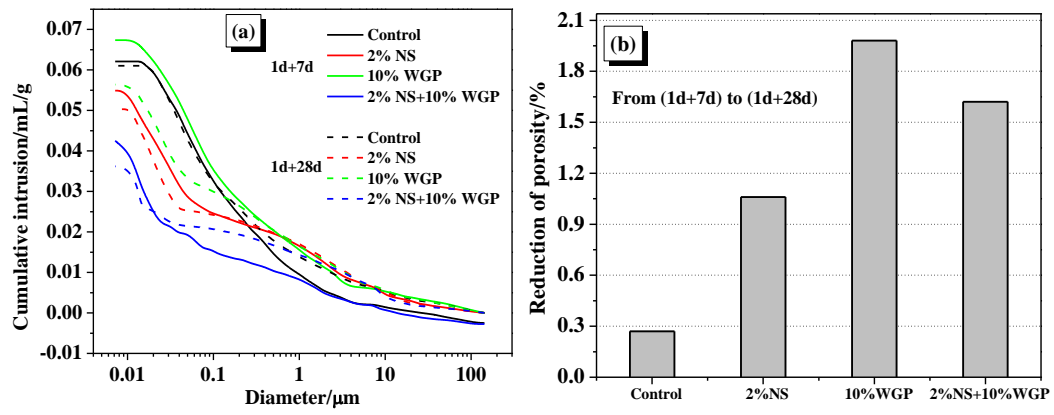Fig. 7 Compressive strengths of cement mortars exposed to ASR test

Fig. 8 Pore size distribution of cement mortar experienced to the accelerated ASR test for (1d+7d)

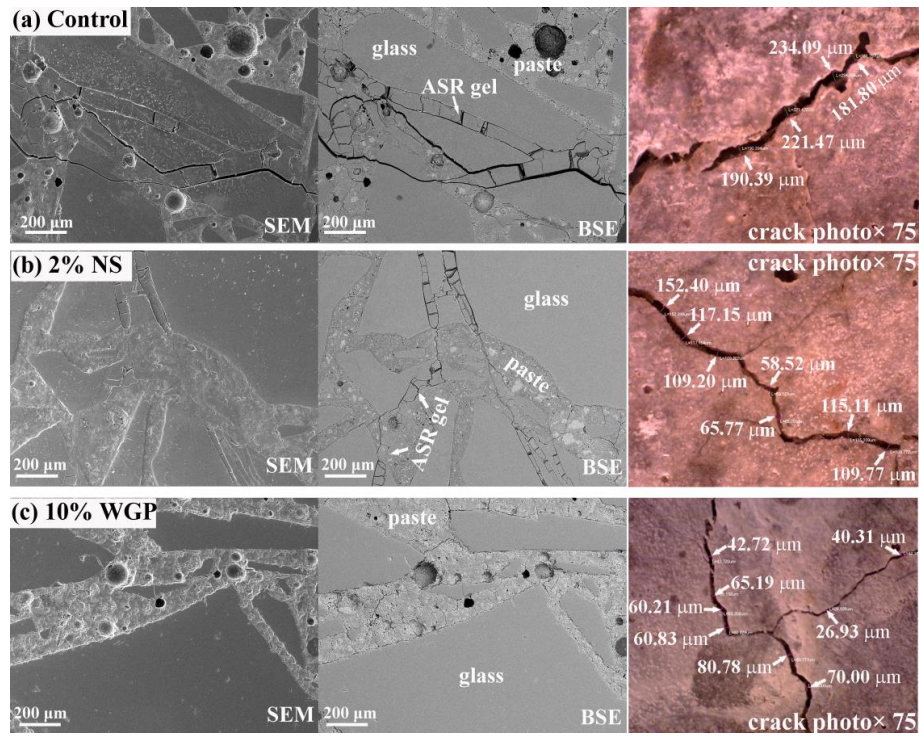and (1d+28d) (a) and the reduction in porosity from (1d+7d) to (1d+28d) (b)

Fig. 9 SEM images (left), BSE images (middle) and crack photos (right) of mortars after subjecting to accelerated ASR test for (1 d + 28 d) ((a): control; (b): 2% NS; (c): 10% WGP)
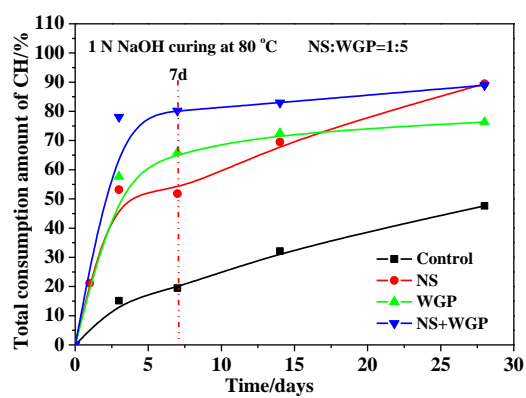
Fig. 10 Consumption of Ca(OH)$_2$ by NS or WGP (NS:WGP=1:5)